ORIGINAL PAPER
Polish Journal of Microbiology
2023, Vol. 72, No 1, 47–60
https://doi.org/10.33073/pjm-2023-009

Chlorine Dioxide Reprograms Rhizosphere Microbial Communities to Enrich Interactions with Tobacco (*Nicotiana tabacum*)

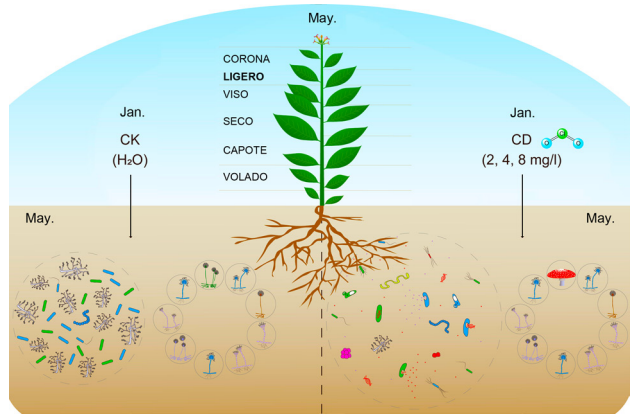
SHI QI[1], JILI ZHANG[2], XINBO LUAN[1], JUNLIN LI[3], ZIKANG HE[1], JUNRU LONG[1], MENGYUN XU[1], PING LI[1], ZEPENG CHEN[4], JIANYU WEI[2]* and JIAN YAN[1]*

[1] Key Laboratory of Agro-Environment in the Tropics, Ministry of Agriculture and Rural Affairs; Guangdong Provincial Key Laboratory of Eco-Circular Agriculture; Guangdong Engineering Research Centre for Modern Eco-Agriculture; College of Natural Resources and Environment, South China Agricultural University, Guangzhou, China
[2] China Tobacco Guangxi Industrial Company Limited, Nanning, China
[3] Guangxi Tobacco Baise Industrial Company Limited, Baise, China
[4] China Tobacco Guangdong Industrial Company Limited, Guangzhou, China

Submitted 25 November 2022, accepted 10 February 2023, published online 24 March 2023

Abstract

For decades chlorine dioxide has been used in water disinfection with excellent results. As the scope of application expands, chlorine dioxide has the potential for soil disinfection. We used amplicon sequencing and gas chromatography-mass spectrometry to compare the changes of four mixed rhizosphere microbial community samples and 12 tobacco leaf volatile samples four months after the flood irrigation with chlorine dioxide in different concentrations (0, 2, 4, 8 mg/l). Phenotypic data of 60 tobacco plants were also collected. The effects of chlorine dioxide on rhizosphere microorganisms were positively correlated with dose gradients. Bacteria responded more strongly in both community structure and metabolic pathways than fungi. Five new bacterial phyla (Firmicutes, Bacteroidota, Myxococcota, Patescibacteria, Verrucomicroboata) appeared in chlorine dioxide treatment groups, while the fungal community only appeared as one new fungal phylum (Basidomycota). Alterations in 271 predicted metabolic bacterial pathways were found. However, in the fungal community were only 10 alternations. The correlations between leaf volatile compounds and rhizosphere microorganisms under the influence of chlorine dioxide treatment could be observed based on network results. However, natural connectivity had already been declining rapidly when less than 20% of the network's nodes were removed. Therefore, the microbe-metabolite network is not stable. It might be why chlorine dioxide treatments did not significantly affect tobacco quality ($p = 0.754$) and phenotype ($p = 0.867$). As a comprehensive investigation of chlorine dioxide in agriculture, this study proves the effectiveness and safety of chlorine dioxide soil disinfection and widens the application range of chlorine dioxide.



K e y w o r d s: chlorine dioxide, soil disinfection, rhizosphere microbiome, plant-microbe interactions, *Nicotiana tabacum*

Introduction

Due to its high efficiency, chemical control has been widely used to prevent rhizosphere-mediated disease (Panth et al. 2020). However, some chemicals are harmful to humans or the environment, thus limiting their application potential to the extent (Ristaino and Thomas 1997; Pesonen and Vähäkangas 2020).

Chlorine dioxide (ClO_2) is a strong oxidant with broad antimicrobial spectrum, non-toxic to human

* Corresponding author: J. Yan, Key Laboratory of Agro-Environment in the Tropics, Ministry of Agriculture and Rural Affairs; Guangdong Provincial Key Laboratory of Eco-Circular Agriculture; Guangdong Engineering Research Centre for Modern Eco-Agriculture; College of Natural Resources and Environment, South China Agricultural University, Guangzhou, China; **e-mail: yanjian78@scau.edu.cn**
J. Wei, China Tobacco Guangxi Industrial Company Limited, Nanning, China; **e-mail: jtx_wjy@163.com**
© 2023 Shi Qi et al.
This work is licensed under the Creative Commons Attribution-NonCommercial-NoDerivatives 4.0 License (https://creativecommons.org/licenses/by-nc-nd/4.0/).

body, and does not pollute the environment (Gómez-López et al. 2009; Zhong et al. 2019; Jefri et al. 2022). Therefore, it plays a vital role in tap water and sewage treatment (Aieta and Berg 1986; Katz et al. 1994), medical apparatus and environment disinfection (Lowe et al. 2013; Meyers et al. 2020), and food preservation (Park and Kang 2015; Sun et al. 2017). After 12 hours of exposure to chlorine dioxide gas (4 mg/l, 0.16 mg/g), the number of yeasts, molds, *Listeria monocytogenes*, *Salmonella* spp., and *Escherichia coli* O157:H7 decreased by 3.10, 3.17, 3.94, 3.62, and 4.25 logs CFU/g, respectively (Popa et al. 2007). The antimicrobial mechanism of chlorine dioxide is the theoretical basis of application. Chlorine dioxide increases the permeability of the bacterial outer membrane and the bacterial plasma membrane, causing electrolyte leakage and eventually killing the bacteria (Ofori et al. 2018). In addition, chlorine dioxide destroys the fungal cell membrane's integrity and leads to death of fungi (Liu et al. 2020). The reaction environment in the soil is complex, which may affect the effectiveness of chemical pesticides. For example, the lower the pH, the weaker the disinfection effect of the chlorine dioxide solution. An alkaline environment is the most suitable for chlorine dioxide reactions (Ofori et al. 2018). In addition, organic matter can absorb gaseous chlorine dioxide (Ramsey and Mathiason 2020) and react with chlorine dioxide solution (Hassenberg et al. 2017). These conditions should be considered when determining the dosage of chlorine dioxide.

The application of gaseous chlorine dioxide to soil disinfection has been well studied. A field study applied to the control of *Phytophthora ramorum* showed that the maximum proportion of gaseous chlorine dioxide inactivating pathogens was 82%. Meanwhile, the disinfection efficiency increased with the soil moisture (Layman et al. 2020). Greenhouse studies indicated that the maximum *Bacillus subtilis* spores log10 reduction was 4.12 and 5.82 for the play sand and the mixed soil, respectively. In addition, as gaseous chlorine dioxide is denser than air, its concentration at the bottom was 3.8 and 3.95 times higher than at the top of the play sand and the mixed soil, respectively (Ramsey and Mathiason 2020). Since the solution is an important form of pesticide use, soil disinfection with chlorine dioxide solution is also worth studying. How does it currently perform in agricultural production? More importantly, is it safe for crops? These problems are closely related to the potential application strategy of chlorine dioxide solution in agriculture.

There are complex interactions between soil microbes and plants (Trivedi et al. 2020). Plants alter their root exudates to recruit rhizosphere microorganisms as the first barrier against soil-borne pathogens (Mendes et al. 2011; Liu et al. 2021; Song et al. 2021). Soil pathogens can also evade or suppress the plant's immune system to infect the host (De Jonge et al. 2010; Sánchez-Vallet et al. 2013; Gao et al. 2019). Therefore, rhizosphere microorganisms deserve attention. Since tobacco leaves are rich in volatile compounds (Zhang et al. 2013) and become even more abundant after flue-curing (Wahlberg et al. 1977), it is suitable for non-target metabolome analysis of the effects of chlorine dioxide on plant quality. Hence, tobacco was chosen as an indicator crop.

With these ideas in mind, we designed experiments combining amplicon sequencing and gas chromatography-mass spectrometry with studying the effects of chlorine dioxide soil disinfection on rhizosphere microbial communities and plants. We ask the following questions: 1) whether and how does chlorine dioxide solution affects rhizosphere microbial communities? 2) whether and how chlorine dioxide solution affects crops?

Experimental

Materials and Methods

Field experiments. Before tobacco seedlings were transplanted, the field experiment was conducted in Guolao Village, Baise City, Guangxi Province, China (23°02′N, 106°35′E) in January 2021. According to the Baise Climatological Survey, the average air temperature ranges from 19.0°C to 22.1°C, and the annual precipitation was 1,114.9 mm. The soil type is paddy, slightly acidic (pH 5.06), and the organic matter content is 34.35 g/kg (Table SI). Tobacco-Rice Rotation is common there; each 20-m^2 plot was planted with 40 tobaccos during the experiment. On the flat terrain, plots were distributed in three completely randomized blocks. Each block contained four plots (one control, three treatments). To ensure adjacent plots keep isolated, 0.8 m width ridges were built around them. In addition, plots in the same block were about 1 m apart, and the distance between neighboring blocks was no less than 2 m. The control plot was flood irrigated with 2,000 l of tap water (0 mg/l), equal to the chlorine dioxide solution used in other plots. The commercial powder formulation of chlorine dioxide (HS Pharma, China), consisting of passivated sodium chlorite and acid, with an active ingredient (malonic acid-iodimetry method) of 10% ± 1%, was applied in a half (powder concentration 20 mg/l, effective chlorine dioxide content 2 mg/l), in a normal (powder concentration 40 mg/l, effective chlorine dioxide content 4 mg/l) and in a twofold dose (powder concentration 80 mg/l, effective chlorine dioxide content 8 mg/l). To prevent the lack of acidic environment resulting in sodium chlorite reaction yield reduction, the mother liquor (effective chlorine dioxide content 2,000 mg/l) was first prepared in a ratio of 20 g powder to 1 l tap water and then

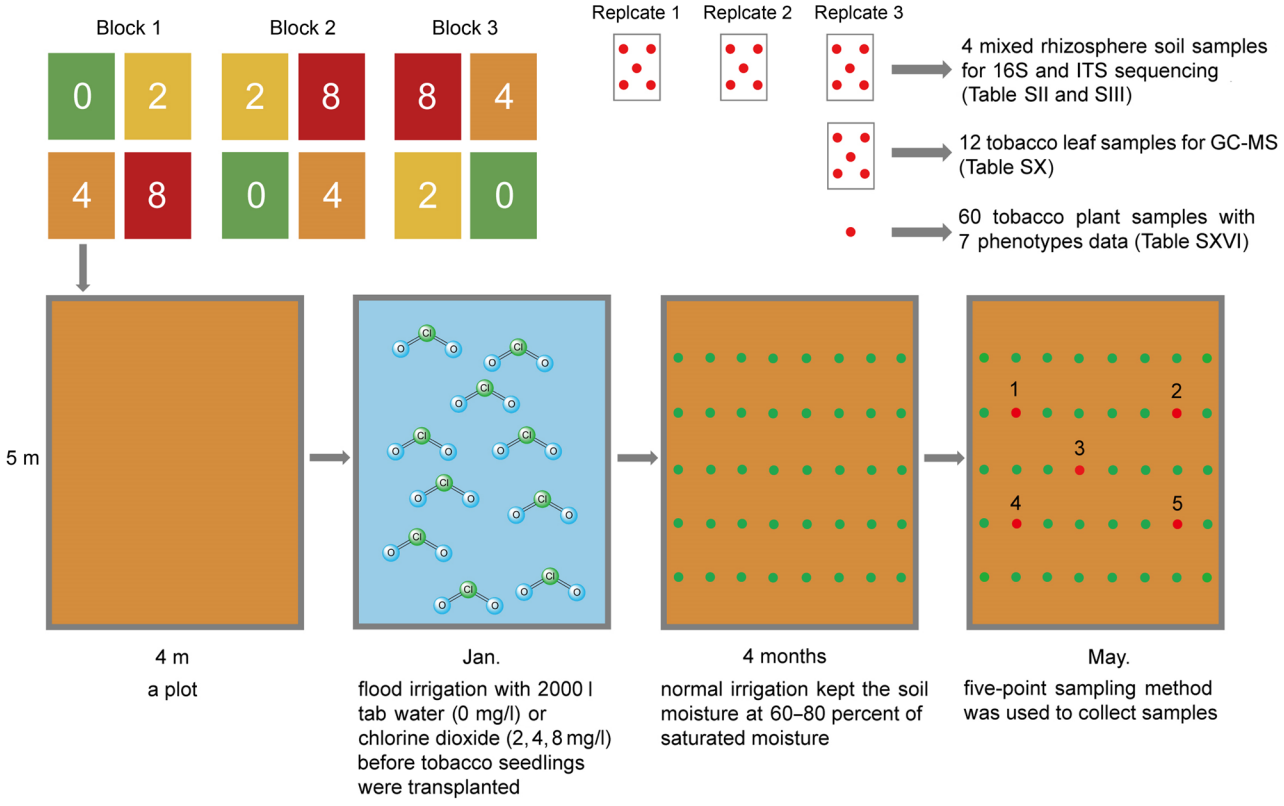


Fig. 1. Summary of experimental design.

diluted to the required concentration in a plastic tank. We used chlorine dioxide quick test paper on-site to detect the concentration and confirm that the actual content conforms to the experimental design. Regular irrigation for the next four months kept the soil moisture at 60–80 percent of saturated moisture (Fig. 1).

16S rRNA and ITS amplicon sequencing. Before tobaccos were harvested, 12 rhizosphere soil samples were collected from 12 plots with a five-point sampling strategy in May 2021. The soil auger used was 2.5 cm in diameter and 15 cm in depth. After getting enough roots with a soil auger, we shake off the loose soil from the roots and use a small brush to collect the rhizosphere soil tightly attached to the root. Three parallel soil samples of equal weight were mixed well with the sterile mortar and pestle. Three grams of the mixing sample of the group were taken. To obtain soil microbial DNA, 1 g of each mixed sample was used for extraction with the E.Z.N.A.® Soil DNA kit (D5625, Omega Bio-tek Inc., USA). All operations were performed following the manufacturer's protocols. To assess the DNA quality, OD 260/230 nm and OD 260/280 nm values were measured by the NanoDrop™ 2000 Spectrophotometer (Thermo Fisher Scientific, USA). For each sample, 260/230 ratio was larger than 1.7, and 260/280 ratio was larger than 1.8.

Ten ng of DNA was used for PCR amplification (20 µl reaction, 30 cycles) in triplicate. In detail, primer sets 338F/806R, and ITS1F/ITS2R were used to amplify the 16S rRNA V3-V4 region gene and the ITS1 region gene. After that, the amplified products were sequenced with the 2 × 300 bp kit using the Illumina MiSeq platform at the Majorbio Corporation (China).

Gas Chromatography-Mass Spectrometry. Along with rhizosphere soil samples, 12 ligero leaf samples were collected with a five-point sampling strategy in May 2021. We collected the top four pieces of tobacco leaf with the stem and flue-cured them in the tobacco curing room. The third leaf from the top was chosen as the sample. These plant materials were frozen in the −80°C refrigerator before use. During pre-treatment, 50 mg of each sample was taken for immersing with liquid nitrogen and powdering using a grinding machine (LUKYM24, China). A mixture of methanol and dichloromethane (3:2) was added into the centrifuge tube containing samples to extract at 50 mg/ml concentration. After 10 min of ultrasonic treatment (KL-040ST, China) at room temperature (25°C), the supernatant was filtered through 0.22 µm membrane filtration. 200 µl of the solution was transferred to the sample bottle prepared for GC-MS analysis.

GC conditions: A Hp-5 (Agilent 19091J-413) column (30 m × 0.25 mm × 0.25 µm) (Agilent, USA) was used; the injection port temperature was 250°C. The column temperature was programmed as follows: the initial temperature at 80°C (held for 5 min), increased to 100°C at 2°C/min, increased to 180°C at 5°C/min (held for 1 min), increased to 200°C at 2°C/min, increased to 280°C at

10°C/min (held for 15 min). The injection volume of filter liquor was 0.5 µl. High-purity helium was utilized as the carrier gas. The gas flow rate was set as 1.0 ml/min.

MS conditions: An electron ionization (EI) ion source was used with 70 EV ionization energy. The mass spectra scanning range was set as 30 ~ 500 m/z. The ion source temperature was 230°C, and the GC/MS interface temperature was 280°C.

Data processing: NIST 2014 was used in the matching comparison. The screening criteria was that the matching rate should be more than 600. The relative content of each component was presented by peak area.

Bioinformatic and statistical analyses. Fastp 0.23.0 (Chen et al. 2018) was used to trim the adaptor and remove low-quality and short reads. Microbiome data were analyzed by QIIME2-2021.11 (Bolyen et al. 2019). With the q2-demux plugin, quality control and demultiplexing of FASTQ files were performed. After that, DADA2 (Callahan et al. 2016) denoising was performed using the q2-dada2 plugin. To align every ASV, mafft (Katoh and Standley 2013) was used through the q2-alignment plugin. Then, via the q2-phylogeny plugin, the phylogenetic tree was constructed with fasttree2 (Price et al. 2010). Assigning ASVs to bacteria and fungi was performed through the q2-feature-classifier (Bokulich et al. 2018) plugin, which used Scikit-learn naive Bayes classifier, against the Sliva 138 database (Quast et al. 2012) and UNITE reference sequences (Nilsson et al. 2019), respectively.

Subsequent analyses of taxon abundances were principally conducted in R software (version 4.1.3) (R Core Team 2013). Bacterial and fungal ASVs abundance tables were resampled to a median of 4,910 and 10,940 reads per sample using the phyloseq R package (McMurdie and Holmes 2013). The Newick trees were visualized using table2itol (freely available in https://github.com/mgoeker/table2itol) and Interactive Tree Of Live version 5 (Letunic and Bork 2021). In addition, Canberra dissimilarity between control and disinfectant microbial communities was measured within the R library vegan (Oksanen et al. 2013), and the construction and visualization of a hierarchical clustering tree (UPGMA) were accomplished using ggtree (Yu et al. 2017).

Due to the ability of PICRUSt2 software (Douglas et al. 2020) to predict metabolic pathways according to taxonomy annotation of ASVs, the calculation of metabolic pathways and orthologs abundances was executed in default settings. We wrote a script of Python 3 to analyze predicted MetaCyc pathways (Caspi et al. 2020), and its visualization was accomplished using the R package networkD3 (freely available at https://christophergandrud.github.io/networkD3). We developed an R script to analyze predicted KEGG ortholog (KO) and significantly differentially abundant KOs ($|\log2FC| > 1$, $p < 0.01$) visualization was accomplished using the R package ggplot2 (Kanehisa and Goto 2000). KEGG pathway enrichment analysis was performed using the R package Clusterprofile (Wu et al. 2021).

To unveil microbe-plant links possibly caused by chlorine dioxide, we developed a co-occurrence network analysis R script. All networks were constructed based on Spearman correlations between normalized family abundances of rhizosphere soil microorganisms, and metabolite abundances of ligero leaves measured by GC-MS (absolute correlation ≥ 0.8, p-value ≤ 0.1). Network visualization was accomplished by Gephi version 0.9.2 (Bastian et al. 2009). Using the R package igraph version 1.2.11 (Csardi and Nepusz 2006), various network topological indices were calculated to characterize the topological structure of co-occurrence networks: modularity, degree, weight degree, closeness centrality, betweenness centrality, eigenvector centrality. In addition, within-module connectivity, among-module connectivity, and network stability comparison were calculated by another R script. Principal coordinates analyses (PCoA) on basis of Bray-Curtis distance of the node topological properties matrix was performed within the R library vegan (Oksanen et al. 2013). A natural connectivity analysis was carried out using an R script to analyze network robustness. According to the importance of nodes in the network, nodes were removed in order. At the same time, the natural connectivity of the incomplete network was computed. The trend of value variation could reflect the robustness of the network.

During the flood irrigation, plastic tanks used as water sources were placed on the side of the road. To analyze the relationship between the inlet distance of flood irrigation and tobacco phenotype, we selected 16 tobacco plants from four plots for the t-test (Fig. S1).

Results

Bacterial and fungal communities. We analyzed the soil microbiome by 16S rRNA and ITS amplicon sequencing to investigate whether the rhizosphere microorganisms changed with chlorine dioxide dose. All bacterial and fungal communities were influenced by chlorine dioxide treatment (Fig. 2). Diversities of each treatment group were higher than the control group. At the same time, the change degree was lower in fungal communities than in bacterial communities. In addition, changed microorganisms also remained stable. Thus, the most abundant several taxa kept the same order along with increasing chlorine dioxide. Hierarchical clustering results revealed that the difference between the blank group and the treatment group was more significant in bacterial microbiome (Fig. 3).

Bacterial and fungal functional potential. To evaluate the potential function of rhizosphere microbial

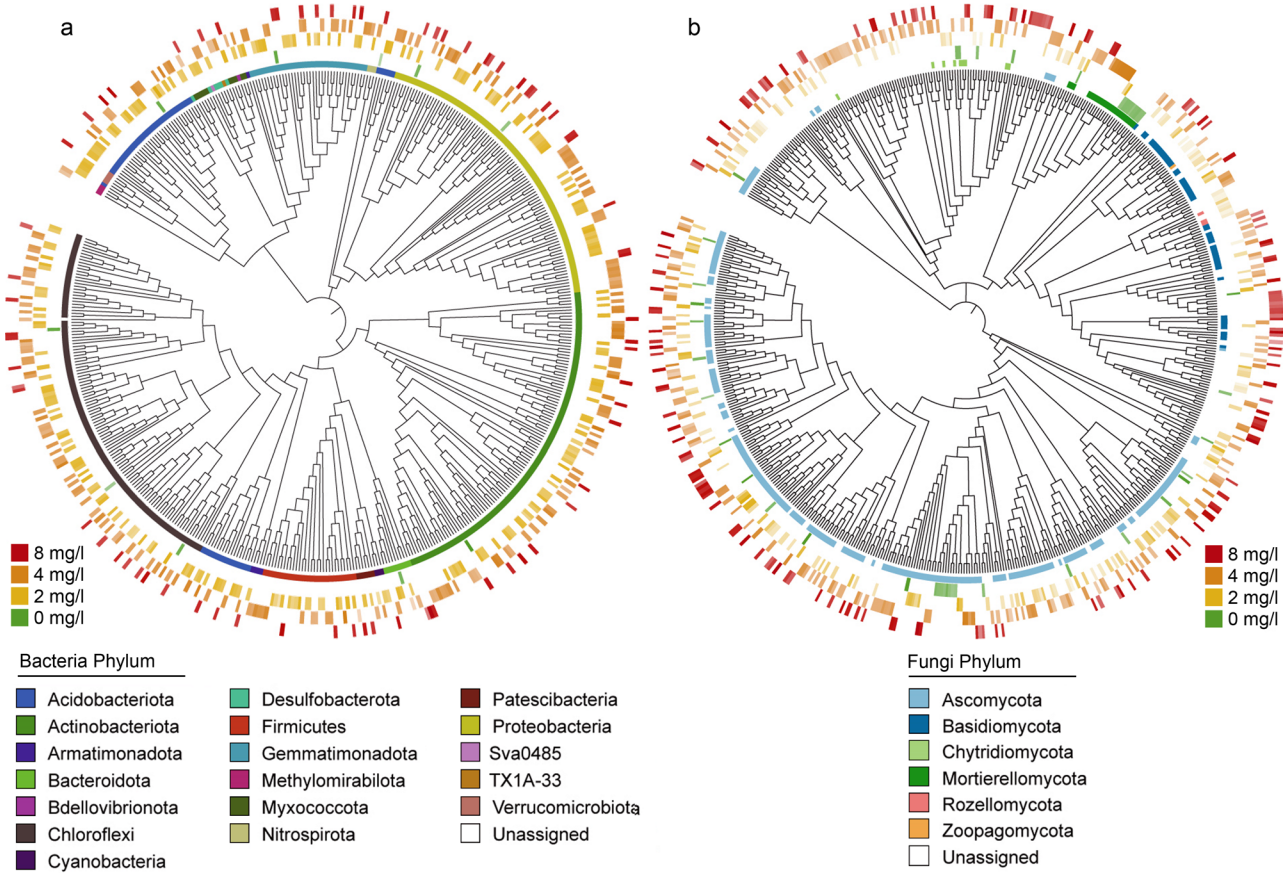


Fig. 2. ASVs found in a) bacterial and b) fungal microbiomes of different groups.
From inside to outside: taxonomic dendrogram showing each group's bacterial and fungal microbiome. The first color ring identifies microbial phyla within the rhizosphere soil. Other color rings represent the relative abundance of ASVs in different groups.

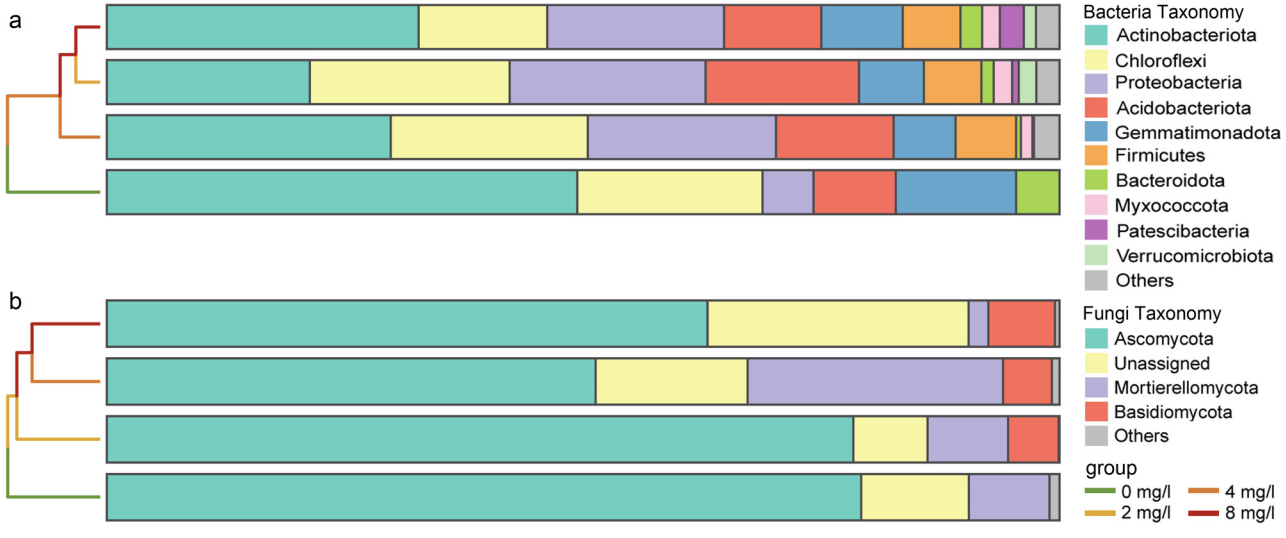


Fig. 3. Taxonomy of a) bacterial and b) fungal microbiome in different groups.
Phyla that accounted for less than 0.6% of total abundance within the four groups were classified as "Others".

communities, we used PICRUSt2 to calculate the abundances of metabolic pathways and orthologs. Corresponding to the changes in the diversity of the microbial community, bacterial metabolic pathways changed significantly, and fungal pathways remained relatively stable (Fig. 4). Alterations in 271 predicted metabolic bacterial pathways were found. These pathways belonged to the bacterial MetaCyc biosynthesis (n = 137), degradation/utilization/assimilation (n = 32), generation of precursor metabolites and energy (n = 33), superclasses (n = 67), and others (n = 2). Almost half (44.57%) of bacterial metabolic pathways were changed,



Fig. 4. Alteration of predicted metagenomic pathways in a) bacterial and b) fungal microbiome.

UP – $p < 0.05$, log2FC > 1; DOWN – $p < 0.05$, log2FC < –1; STABLE – p > 0.05 or –1 < log2FC < 1; D/U/A – Degradation/Utilization/Assimilation; GoPMaE – Generation of Precursor Metabolites and Energy. One-sample *t*-test was used to evaluate the significance of differences between the control and treatment groups.

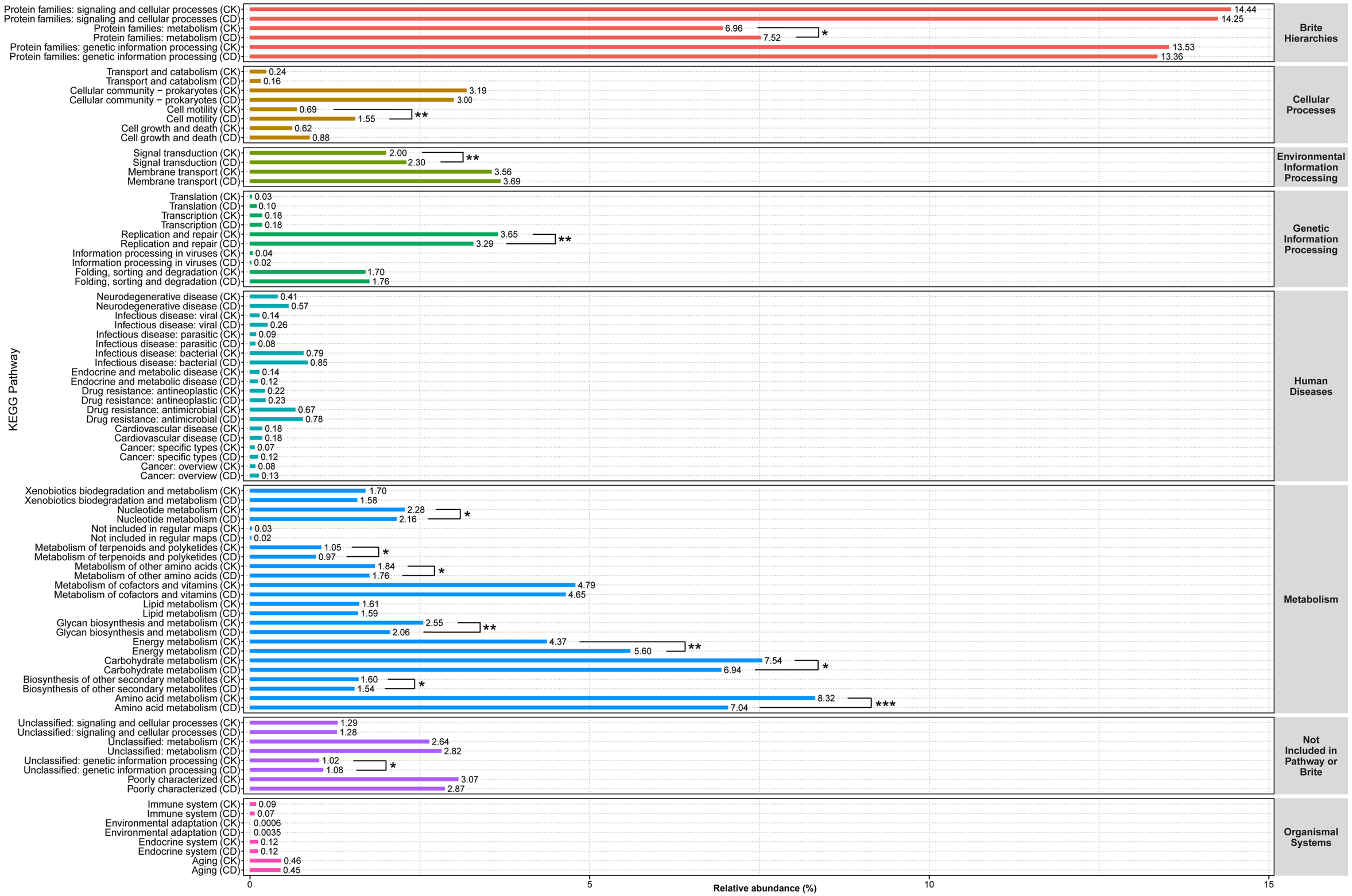


Fig. 5. Relative abundance of bacterial KEGG pathways in levels 1 and 2.

CK – H_2O treatment; CD – chlorine dioxide treatment.

* $0.01 < p \leq 0.05$; ** $0.001 < p \leq 0.01$; *** $p \leq 0.001$.

One-sample *t*-test was used to evaluate the significance of differences between the control and treatment groups.

and nearly all (98.89%) of them increased in number (Table SIV and SV). Alterations in 10 predicted metabolic fungal pathways were found. These pathways belonged to the fungal MetaCyc biosynthesis (n = 2), degradation/utilization/assimilation (n = 4), generation of precursor metabolites and energy (n = 1), and superclasses (n = 3). Only a small number (8.13%) of fungal metabolic pathways were changed, and all increased in number (Table SVI and SVII).

Further analysis of bacteria was conducted with the KEGG Pathway database. 29.54% of level 2 pathways were significantly changed (Fig. 5). A comparison of KEGG ortholog (KO) abundance led to the identification of 1612 KOs with different abundance. Of these, 1,377 genes increased, and 235 genes decreased in abundance (Table SVIII). Many KOs were missing as few in the control group, which resulted many asymmetric points with high fold-change values (Fig. 6a).

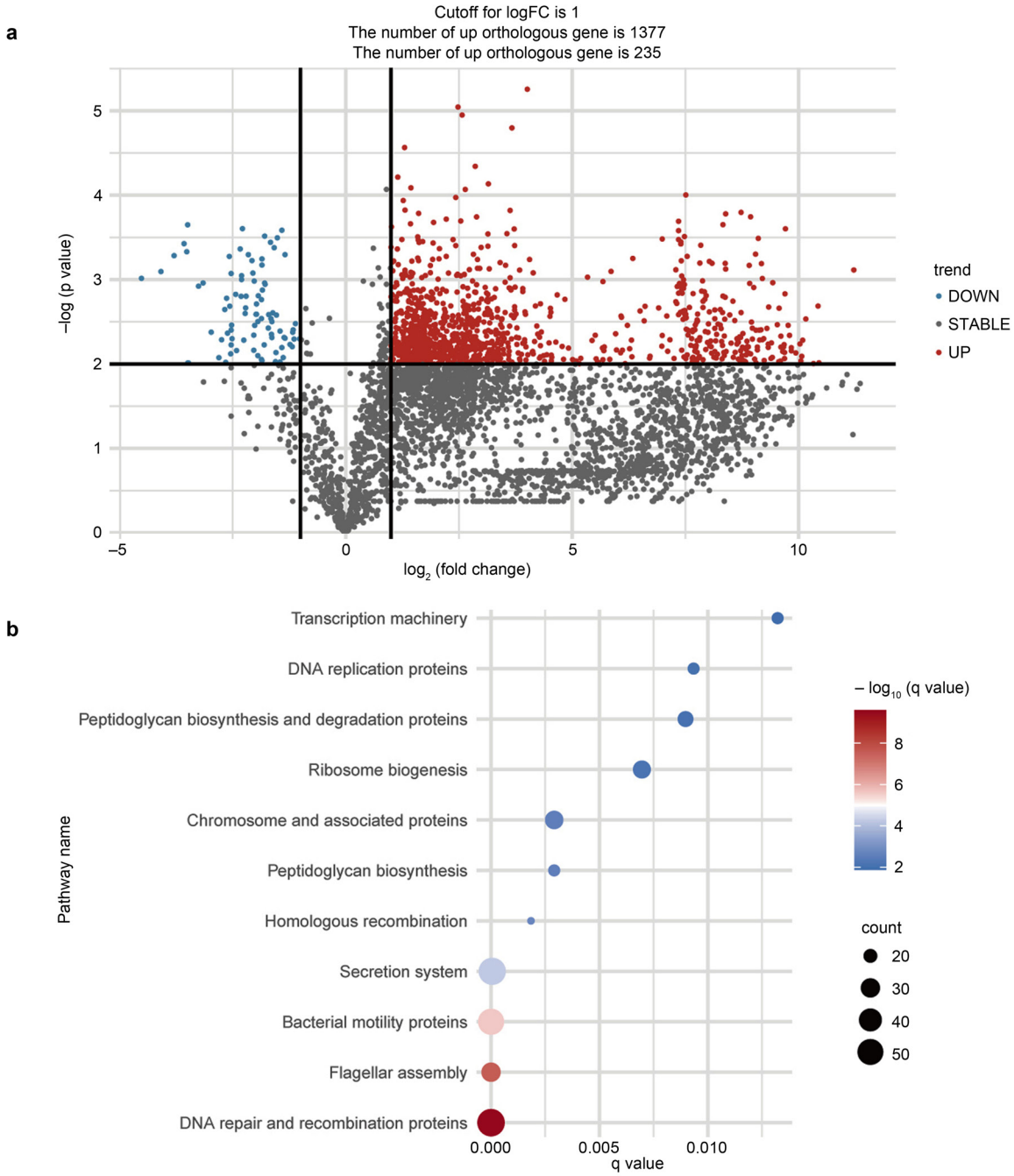


Fig. 6. KEGG enrichment analysis of bacterial communities.

a) Volcano plots of DEGs between the control and the treatment group. The horizontal and vertical lines indicate a significance threshold ($p < 0.01$, $|\log2FC| > 1$). Red dots represent upregulated DEGs, and blue dots represent downregulated DEGs.

b) Bubble diagram of the upregulated and downregulated DEGs in the KEGG database. The size of a bubble represents the number of DEGs. The color of a bubble represents the enrichment value of DEGs. One-sample *t*-test was used to evaluate the significance of differences between control and treatment groups.

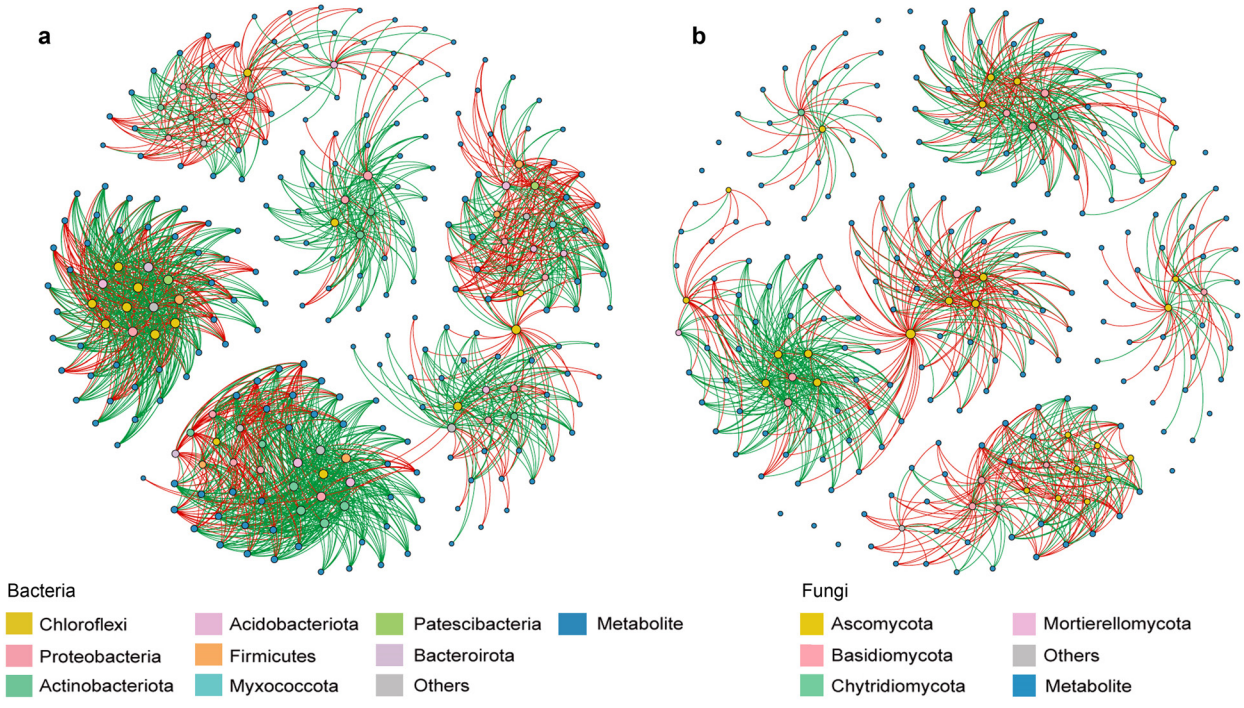


Fig. 7. Visualization of the a) bacteria-metabolite and the b) fungi-metabolite network.
Network construction is based on Spearman correlation calculation results. Blue dots represent volatile compounds. The other dots represent different family-level microbial taxonomy, respectively. Bacterial dots with different colors represent different bacterial phyla. Fungal dots with different colors represent different fungal phyla. Red lines represent positive correlations, and green lines represent negative correlations (absolute correlation ≥ 0.8, p-value ≤ 0.1).

The KEGG analysis showed that many movement-related, reproduction-related, and metabolism-related pathways were significantly enriched, which was similar to the results of bacterial MetaCyc metabolic pathways (Fig. 6b and Table SIX).

Microbe-metabolite networks. We employed a co-occurrence network analysis to assess the effects of the rhizosphere microbial community on the volatile component of tobacco leaves under the influence of chlorine dioxide. Bacteria-metabolite network was denser than the fungi-metabolite network. There were more negative correlations in the bacteria-metabolite network. Meanwhile, metabolite and microbial nodes appeared with different distribution regularities in the network. Within the same module, metabolite nodes were distributed along the edge all the time, and microbe nodes always were located in the center (Fig. 7). All 207 metabolites were correlated with bacteria. In contrast, 11 of these were not correlated with fungi. In addition, 66 bacterial families and 40 fungal families exist in the network, which accounted for 56.4% of all 117 bacterial families and 59.7% of all 67 fungal families (Table SX, SXI, and SXII).

In addition to distribution regularity, metabolite and microbial nodes they also had different topological properties. The degree of metabolite nodes was usually lower than microbe nodes. Among-module connectivity of metabolite nodes was often greater, while within-module connectivity showed an opposite trend. Thus, metabolite nodes always were connectors, and module hubs always were microbe nodes (Fig. 8). PCoA results of node properties showed distribution difference between microbe nodes and metabolite nodes (Table SXIII and SXIV, Fig. 9a and 9b). Natural connectivity analysis suggested that the robustness of microbe-metabolite networks was fragile, although their trends slightly differed (Fig. 10a). PCoA results of volatile metabolite showed no significant difference between the groups (Fig. 10b). PCoA results of tobacco phenotype demonstrated no significant differences among the groups (Fig. 10c). According to the t-test results, the distance from the entrance of flood irrigation had no significant effect on the phenotype of tobacco plants ($p > 0.05$) (Fig. S4).

If we define phyla that appeared in the taxa bar after chlorine dioxide treatment as a "new-phylum", bacterial new-phyla (Firmicutes, Bacteroidota, Myxococcota, Patescibacteria, and Verrucomicroboata) accounted for 11.3% of the bacterial community. Fungal new-phylum (Basidomycota) accounted for 5.8% of the fungal community (Table SII and SIII). However, according to the importance of nodes in the network, four of ten nodes (40%) removed from the bacteria-metabolite network belonged to bacterial new-phylum, and three of ten nodes (30%) removed from the fungi-metabolite network belonged to fungal new-phylum (Table SXV).

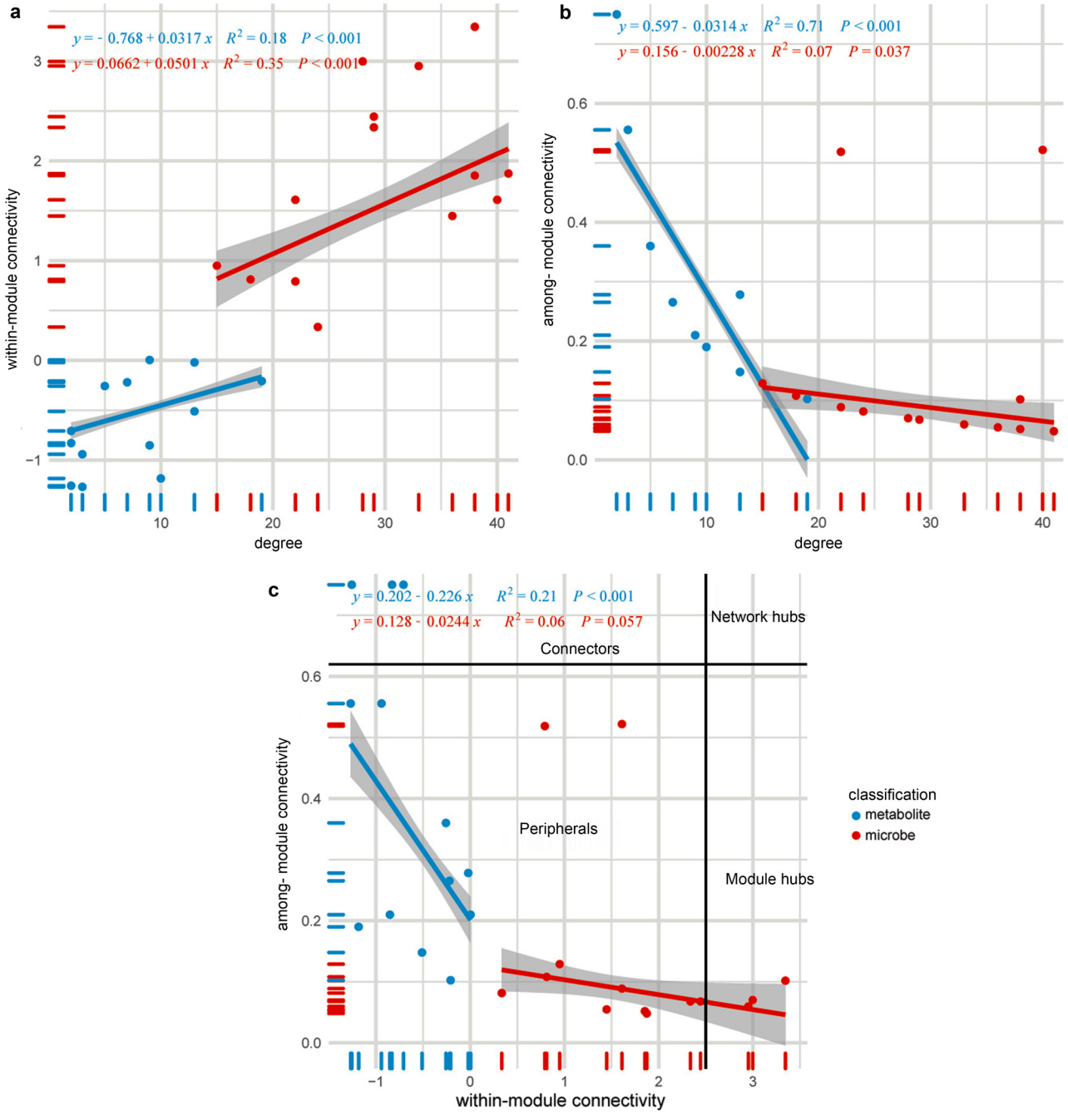


Fig. 8. Relationships among partial network node attributes.

a), d), Relationships between degree and within-module connectivity (Z_i) in a) bacteria-metabolite and d) fungi-metabolite network; b), e), relationships between degree and among module-connectivity (P_i) in b) bacteria-metabolite and e) fungi-metabolite network; c), f), keystone taxa were speculated based on their topological node features in c) bacteria-metabolite and f) fungi-metabolite network. Blue dots represent metabolite nodes, and red dots represent microbe nodes. A node was identified as a module hub if its $Z_i \geq 2.5$, as a connector if its $P_i \geq 0.62$, and as a network hub if it had $Z_i \geq 2.5$ and $P_i \geq 0.62$. *F*-tests were performed to evaluate whether models could adequately describe the data.

Discussion

According to microbial community structure and function analysis results, chlorine dioxide had an effect on rhizosphere microorganisms, and the effect on microbial community structure was enhanced with the increase of the dose (Fig. 2, 3, and 4). The disinfection treatment was only carried out once before transplanting, while the effects were not eliminated when the tobacco was harvested. KEGG enrichment analysis of rhizosphere bacterial communities revealed more details of the stress response. Chlorine dioxide might induce chemotaxis in soil bacterial community. Flood irrigation brings excess water, and soil pores are filled with water, while soil particles are less affected (Haghnazari et al. 2015). Because of chemotaxis, bacteria

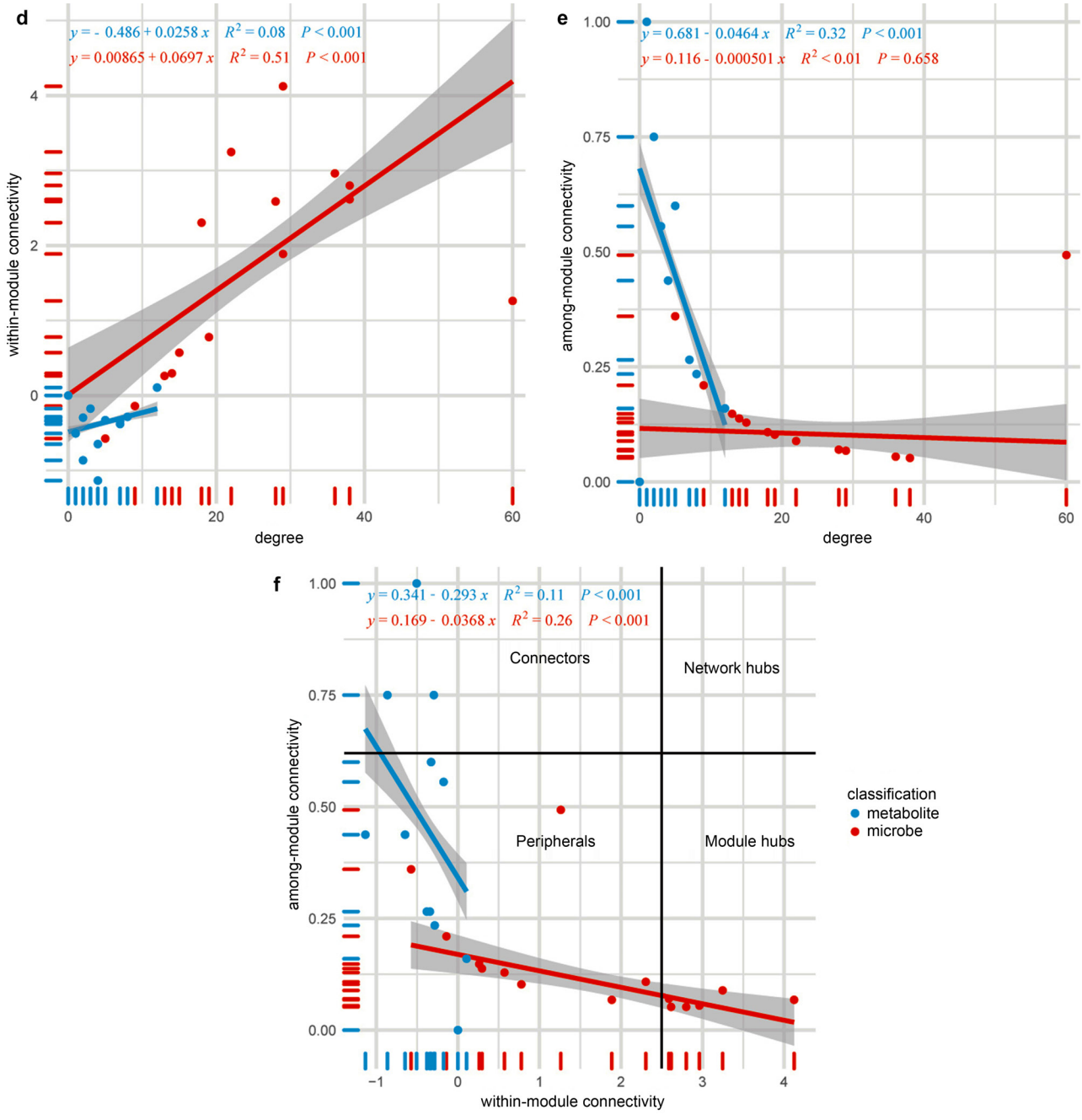


Fig. 8. Relationships among partial network node attributes.

a), d), Relationships between degree and within-module connectivity (Z_i) in a) bacteria-metabolite and d) fungi-metabolite network; b), e), relationships between degree and among module-connectivity (P_i) in b) bacteria-metabolite and e) fungi-metabolite network; c), f), keystone taxa were speculated based on their topological node features in c) bacteria-metabolite and f) fungi-metabolite network. Blue dots represent metabolite nodes, and red dots represent microbe nodes. A node was identified as a module hub if its $Z_i \geq 2.5$, as a connector if its $P_i \geq 0.62$, and as a network hub if it had $Z_i \geq 2.5$ and $P_i \geq 0.62$. *F*-tests were performed to evaluate whether models could adequately describe the data.

tend to escape chlorine dioxide by entering the interior of soil particles. Bacteria with well-developed flagella and strong motility are more likely to survive. Therefore, pathways of flagellar assembly and bacterial motility proteins are enriched in the bacteria kingdom suffering from chlorine dioxide disinfection (Fig. 6b and S2). The peptidoglycan synthesis pathway was also enriched since the P ring of flagellar is embedded in the peptidoglycan layer (Gupta and Gupta 2021) (Fig. 6b and S3). Simultaneous enrichment of flagellar assembly and peptidoglycan synthesis pathways was reported in the transcriptome analysis of the biocide stress effect on *L. monocytogenes* as well (Casey et al. 2014).

Chlorine dioxide might have a better inhibitory effect on bacterial soil-borne diseases. We observed that bacteria respond more strongly than fungi in terms of community structure (Fig. 3) and metabolic pathways (Fig. 4). In addition, pathways related to reproduction

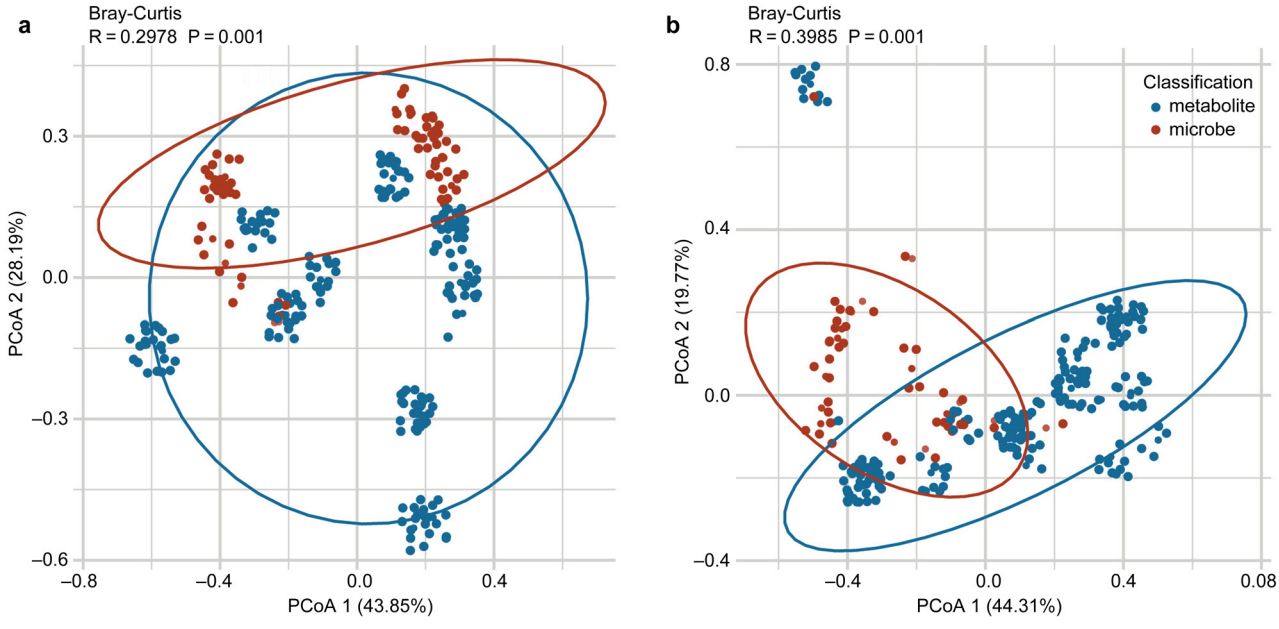


Fig. 9. Node attributes analysis.

Seven topological node parameters in a) bacteria-metabolite and b) fungi-metabolite network (listed in Table SXII and SXIII) were used for a pharmacy curriculum outcomes assessment (PCoA) analysis. Blue dots represent metabolite nodes, and red dots represent microbe nodes. In order to remove the influence of point overlap on observation, a random offset of 0.05 in the horizontal and vertical directions was added to each point. Analyses of similarity (ANOSIM) were performed on the Bray-Curtis distance matrix to evaluate whether there are differences between the metabolite node group and the microbe node group.

were also enriched in the bacterial community after disinfection treatment (Fig. 6). These phenomena suggest that bacteria were sensitive to chlorine dioxide and inactivated massively. As a result, the internal competitive pressure decreased. This difference was consistent with the previous observations that gaseous chlorine dioxide disinfection reduced bacterial concentration levels more than fungi (Popa et al. 2007; Hsu and Huang 2013). We hypothesize that a combination of the antioxidant enzyme and endomembrane systems could explain the different responses of bacteria and fungi to chlorine dioxide. Contemporary microbes inherited iron-dependent enzymes from their anoxic ancestors (Khademian and Imlay 2021). Therefore, oxidative stress induced by reactive nitrogen and oxygen species can also be an immune defense strategy against pathogenic microorganisms (Staerck et al. 2017). Microbes evolved the antioxidant enzyme system to fend off the destructive actions of oxidizing reactions (Khademian and Imlay 2021). Since eukaryotic cells have numerous endomembrane structures which improve the efficiency of cellular physiological and biochemical reactions significantly, tolerance of the antioxidant enzyme system could be better than bacterial one in terms of chlorine dioxide disinfection.

There were correlations between the soil microbial community and volatile tobacco metabolites under the influence of chlorine dioxide. We observed that several enriched pathways (flagella assembly, bacterial motility, bacterial secretion) were also associated with endophytic colonization. Once soil microorganisms perceive plant-derived signals, they move to the root through flagella and attach to the surface. To colonize the plant, they need to form biofilms and produce substances such as microbial detoxification enzymes and lytic enzymes subsequently (Trivedi et al. 2020). Microbe-metabolite co-occurrence network analysis showed that microbe nodes and metabolite nodes are not randomly combined (Fig. 8). In terms of bacteria and fungi, the different modes of topology attributes between two nodes types were also diverse (Fig. 9a and 9b), suggesting potential connections between rhizosphere microorganisms and plant metabolites. In addition, robustness results showed that the association is relatively fragile (Fig. 10a). It may be a reason for the lack of significant difference in tobacco quality and phenotype (Fig. 10b and 10c). Since plants interact with functional traits rather than a taxonomy (Trivedi et al. 2020), functional changes of rhizosphere microbial communities caused by chlorine dioxide might not be enough to affect plants significantly (Fig. 5). Therefore, chlorine dioxide soil disinfection is safe for agricultural application.

According to the ecological community theory, the emergence of "new-phylum" in treatment groups might be the result of "disturbance" and "dispersal" (Vellend 2010). Chlorine dioxide disturbs the soil microbial community, reducing the species' density and making the resources relatively adequate. For the experiment's convenience, the blocks' location was selected near the road, river, and tobacco curing room. Therefore,

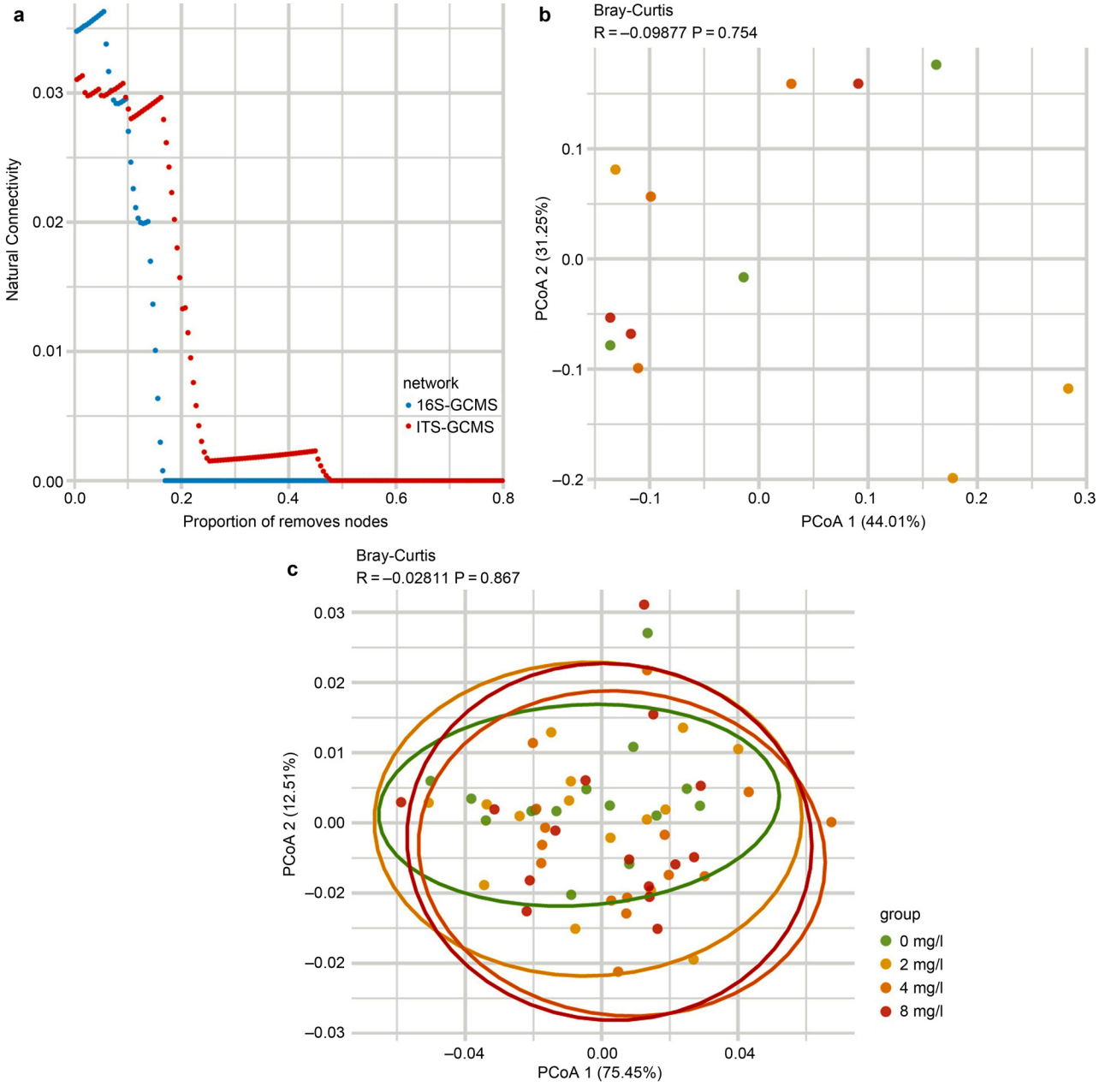


Fig. 10. Network robustness, volatile metabolite, and tobacco phenotype analysis.

a) The natural connectivity of microbe-metabolite networks. Blue dots represent the bacteria-metabolite network, and red dots represent the fungi-metabolite network. b) Abundance of 207 volatile components from 12 plots was used for a pharmacy curriculum outcomes assessment (PCoA) analysis. c) Data on seven phenotypes of 60 tobacco plants were used for a pharmacy curriculum outcomes assessment (PCoA) analysis. The analysis of similarity (ANOSIM) was performed on the Bray-Curtis distance matrix to evaluate whether there are differences between groups.

there was a regional species pool around blocks, and alien species could enter plots through dispersal. In the control group, all the ecological niches were occupied, and colonization by foreign microorganisms was challenging. Treatment groups are the opposite due to the diminished intraspecific and interspecific competition. Plant roots recruited rhizosphere microorganisms from the soil; thus, "new-phylum" appeared in treatment groups. Some beneficial microbes also emerged in treatment groups, such as *Sphingomonas*, which can enhance plant disease resistance (Matsumoto et al. 2021) and nitrogen-fixing *Bradyrhizobium* (Zimmer et al. 2016) (from 0.00% to 0.92%, 1.16%, 1.61%) (Table SII). Newly emerging microbes played a more important role in the network than the resident microorganisms (Table SXV), meaning that they had been screened and filtered through the new environment. Interactions between rhizosphere microorganisms and tobacco were enriched.

There have been some critical studies of chlorine dioxide disinfection in agriculture applications (Layman et al. 2020; Ramsey and Mathiason 2020). We aim to extend their achievements by assessing the effects on the rhizosphere microbial community and plants after

flood irrigation with chlorine dioxide. The advantage of our field experiments is that effects can be evaluated through rhizosphere microbes and crops at different dose gradients. However, a more persuasive mechanism of the presented generalization requires further research with more samples from various sites, using various crops and elucidating temporal variation in soil microorganisms and crop quality.

Availability of data and material

The raw sequences have been deposited with NCBI under the BioProject accession number PRJNA877362.

Acknowledgments

This research was funded by China Tobacco Guangxi Industrial Company Limited, grant number 2020450000340022.

Author contributions

Conceptualization: Z.H. and S.Q.; methodology: J.Y., P.L. and S.Q.; software: S.Q.; validation: J.Y. and J.W.; formal analysis: S.Q.; investigation: Z.H., X.L. and Q.S.; resources: J.Y.; data curation: S.Q.; writing – original draft preparation: S.Q.; writing – review and editing: J.Y., M.X. and J.L.; visualization: S.Q.; supervision: J.Y., J.W., Z.C., J.Z. and J.L; project administration: J.Y.; funding acquisition: J.Y. All authors have read and agreed to the published version of the manuscript.

Conflict of interest

The authors do not report any financial or personal connections with other persons or organizations, which might negatively affect the contents of this publication and/or claim authorship rights to this publication.

Literature

Aieta EM, Berg JD. A review of chlorine dioxide in drinking water treatment. J Am Water Works Assoc. 1986;78(6):62–72. https://doi.org/10.1002/j.1551-8833.1986.tb05766.x

Bastian, M., Heymann, S., & Jacomy, M. Gephi: an open source software for exploring and manipulating networks. Proceedings of the International AAAI Conference on Weblogs and Social Media. 2009;3(1):361–362. https://doi.org/10.1609/icwsm.v3i1.13937

Bokulich NA, Kaehler BD, Rideout JR, Dillon M, Bolyen E, Knight R, Huttley GA, Gregory Caporaso J. Optimizing taxonomic classification of marker-gene amplicon sequences with QIIME 2's q2-feature-classifier plugin. Microbiome. 2018 May;6(1):90. https://doi.org/10.1186/s40168-018-0470-z

Bolyen E, Rideout JR, Dillon MR, Bokulich NA, Abnet CC, Al-Ghalith GA, Alexander H, Alm EJ, Arumugam M, Asnicar F, et al. Reproducible, interactive, scalable and extensible microbiome data science using QIIME 2. Nat Biotechnol. 2019 Aug;37(8):852–857. https://doi.org/10.1038/s41587-019-0209-9

Callahan BJ, McMurdie PJ, Rosen MJ, Han AW, Johnson AJ, Holmes SP. DADA2: High-resolution sample inference from Illumina amplicon data. Nat Methods. 2016 Jul;13(7):581–583. https://doi.org/10.1038/nmeth.3869

Casey A, Fox EM, Schmitz-Esser S, Coffey A, McAuliffe O, Jordan K. Transcriptome analysis of *Listeria monocytogenes* exposed to biocide stress reveals a multi-system response involving cell wall synthesis, sugar uptake, and motility. Front Microbiol. 2014 Feb;5:68. https://doi.org/10.3389/fmicb.2014.00068

Caspi R, Billington R, Keseler IM, Kothari A, Krummenacker M, Midford PE, Ong WK, Paley S, Subhraveti P, Karp PD. The MetaCyc database of metabolic pathways and enzymes – a 2019 update. Nucleic Acids Res. 2020 Jan;48(D1):D445–D453. https://doi.org/10.1093/nar/gkz862

Chen S, Zhou Y, Chen Y, Gu J. fastp: an ultra-fast all-in-one FASTQ preprocessor. Bioinformatics. 2018 Sep;34(17):i884–i890. https://doi.org/10.1093/bioinformatics/bty560

Csardi G, Nepusz T. The igraph software package for complex network research. InterJournal. 2006;1695(5):1–9.

de Jonge R, van Esse HP, Kombrink A, Shinya T, Desaki Y, Bours R, van der Krol S, Shibuya N, Joosten MH, Thomma BP. Conserved fungal LysM effector Ecp6 prevents chitin-triggered immunity in plants. Science. 2010 Aug;329(5994):953–955. https://doi.org/10.1126/science.1190859

Douglas GM, Maffei VJ, Zaneveld JR, Yurgel SN, Brown JR, Taylor CM, Huttenhower C, Langille MGI. PICRUSt2 for prediction of metagenome functions. Nat Biotechnol. 2020 Jun;38(6):685–688. https://doi.org/10.1038/s41587-020-0548-6

Gao F, Zhang BS, Zhao JH, Huang JF, Jia PS, Wang S, Zhang J, Zhou JM, Guo HS. Deacetylation of chitin oligomers increases virulence in soil-borne fungal pathogens. Nat Plants. 2019 Nov; 5(11): 1167–1176. https://doi.org/10.1038/s41477-019-0527-4

Gómez-López VM, Rajkovic A, Ragaert P, Smigic N, Devlieghere F. Chlorine dioxide for minimally processed produce preservation: a review. Trends Food Sci Technol. 2009 Jan;20(1):17–26. https://doi.org/10.1016/j.tifs.2008.09.005

Gupta R, Gupta N. Prokaryotic cell structure and function. In: Fundamentals of bacterial physiology and metabolism. Singapore: Springer; 2021; p. 43–79. https://doi.org/10.1007/978-981-16-0723-3_2

Haghnazari F, Shahgholi H, Feizi M. Factors affecting the infiltration of agricultural soils. Int J Agron Agric Res. 2015;6(5):21–35.

Hassenberg K, Geyer M, Mauerer M, Praeger U, Herppich WBJL-FS. Influence of temperature and organic matter load on chlorine dioxide efficacy on *Escherichia coli* inactivation. LWT Food Sci Technol. 2017 Jun;79:349–354. https://doi.org/10.1016/j.lwt.2017.01.030

Hsu CS, Huang DJ. Disinfection efficiency of chlorine dioxide gas in student cafeterias in Taiwan. J Air Waste Manag Assoc. 2013 Jul; 63(7):796–805. https://doi.org/10.1080/10962247.2012.735212

Jefri UHNM, Khan A, Lim YC, Lee KS, Liew KB, Kassab YW, Choo CY, Al-Worafi YM, Ming LC, Kalusalingam A. A systematic review on chlorine dioxide as a disinfectant. J Med Life. 2022 Mar; 15(3):313–318. https://doi.org/10.25122/jml-2021-0180

Kanehisa M, Goto S. KEGG: Kyoto Encyclopedia of Genes and Genomes. Nucleic Acids Res. 2000 Jan;28(1):27-30. https://doi.org/10.1093/nar/28.1.27

Katoh K, Standley DM. MAFFT multiple sequence alignment software version 7: improvements in performance and usability. Mol Biol Evol. 2013 Apr;30(4):772–780. https://doi.org/10.1093/molbev/mst010

Katz A, Narkis N, Orshansky F, Friedland E, Kott Y. Disinfection of effluent by combinations of equal doses of chlorine dioxide and chlorine added simultaneously over varying contact times. Water Res. 1994 Oct;28(10):2133–2138. https://doi.org/10.1016/0043-1354(94)90024-8

Khademian M, Imlay JA. How microbes evolved to tolerate oxygen. Trends Microbiol. 2021 May;29(5):428–440. https://doi.org/10.1016/j.tim.2020.10.001

Layman ML, Ramsey C, Schweigkofler W, Newman SE. Field evaluation of a novel, granular soil fumigant for controlling *Phytophthora ramorum* in field nursery soils. J Agric Innov Res Dev. 2020 Nov;7:12–19. https://doi.org/10.15377/2409-9813.2020.07.2

Letunic I, Bork P. Interactive Tree Of Life (iTOL) v5: an online tool for phylogenetic tree display and annotation. Nucleic Acids Res. 2021 Jul;49(W1):W293–W296. https://doi.org/10.1093/nar/gkab301

Liu H, Li J, Carvalhais LC, Percy CD, Prakash Verma J, Schenk PM, Singh BK. Evidence for the plant recruitment of beneficial microbes to suppress soil-borne pathogens. New Phytol. 2021 Mar;229(5):2873–2885. https://doi.org/10.1111/nph.17057

Liu X, Jiao W, Du Y, Chen Q, Su Z, Fu M. Chlorine dioxide controls green mold caused by *Penicillium digitatum* in citrus fruits and the mechanism involved. J Agric Food Chem. 2020 Nov; 68(47): 13897–13905. https://doi.org/10.1021/acs.jafc.0c05288

Lowe JJ, Gibbs SG, Iwen PC, Smith PW, Hewlett AL. Impact of chlorine dioxide gas sterilization on nosocomial organism viability in a hospital room. Int J Environ Res Public Health. 2013 Jun; 10(6):2596–2605. https://doi.org/10.3390/ijerph10062596

Matsumoto H, Fan X, Wang Y, Kusstatscher P, Duan J, Wu S, Chen S, Qiao K, Wang Y, Ma B, et al. Bacterial seed endophyte shapes disease resistance in rice. Nat Plants. 2021 Jan;7(1):60–72. https://doi.org/10.1038/s41477-020-00826-5

McMurdie PJ, Holmes S. phyloseq: an R package for reproducible interactive analysis and graphics of microbiome census data. PLoS One. 2013 Apr 22;8(4):e61217. https://doi.org/10.1371/journal.pone.0061217

Mendes R, Kruijt M, de Bruijn I, Dekkers E, van der Voort M, Schneider JH, Piceno YM, DeSantis TZ, Andersen GL, Bakker PA, et al. Deciphering the rhizosphere microbiome for disease-suppressive bacteria. Science. 2011 May;332(6033):1097–1100. https://doi.org/10.1126/science.1203980

Meyers C, Milici J, Robison R. The ability of two chlorine dioxide chemistries to inactivate human papillomavirus-contaminated endocavitary ultrasound probes and nasendoscopes. J Med Virol. 2020 Aug;92(8):1298–1302. https://doi.org/10.1002/jmv.25666

Nilsson RH, Larsson KH, Taylor AFS, Bengtsson-Palme J, Jeppesen TS, Schigel D, Kennedy P, Picard K, Glöckner FO, Tedersoo L, et al. The UNITE database for molecular identification of fungi: handling dark taxa and parallel taxonomic classifications. Nucleic Acids Res. 2019 Jan ;47(D1):D259–D264. https://doi.org/10.1093/nar/gky1022

Ofori I, Maddila S, Lin J, Jonnalagadda SB. Chlorine dioxide inactivation of *Pseudomonas aeruginosa* and *Staphylococcus aureus* in water: The kinetics and mechanism. J Water Process Eng. 2018 Dec; 26:46–54. https://doi.org/10.1016/j.jwpe.2018.09.001

Oksanen J, Blanchet FG, Kindt R, Legendre P, Minchin PR, O'hara R, Simpson GL, Solymos P, Stevens MHH, Wagner H, et al. Package 'vegan'. Community ecology package. 2013;2(9):1–295.

Panth M, Hassler SC, Baysal-Gurel F. Methods for management of soilborne diseases in crop production. Agric. 2020 Jan;10(1):16. https://doi.org/10.3390/agriculture10010016

Park SH, Kang DH. Antimicrobial effect of chlorine dioxide gas against foodborne pathogens under differing conditions of relative humidity. LWT Food Sci Technol. 2015 Jan;60(1):186–191. https://doi.org/10.1016/j.lwt.2014.09.031

Pesonen M, Vähäkangas K. Chloropicrin-induced toxicity in the respiratory system. Toxicol Lett. 2020 May;323:10–18. https://doi.org/10.1016/j.toxlet.2020.01.022

Popa I, Hanson EJ, Todd EC, Schilder AC, Ryser ET. Efficacy of chlorine dioxide gas sachets for enhancing the microbiological quality and safety of blueberries. J Food Prot. 2007 Sep;70(9):2084–2088. https://doi.org/10.4315/0362-028X-70.9.2084

Price MN, Dehal PS, Arkin AP. FastTree 2 – approximately maximum-likelihood trees for large alignments. PLoS One. 2010 Mar; 5(3): e9490. https://doi.org/10.1371/journal.pone.0009490

Quast C, Pruesse E, Yilmaz P, Gerken J, Schweer T, Yarza P, Peplies J, Glöckner FO. The SILVA ribosomal RNA gene database project: improved data processing and web-based tools. Nucleic Acids Res. 2013 Jan;41(D1):D590–D596. https://doi.org/10.1093/nar/gks1219

Ramsey CL, Mathiason C. Novel use of chlorine dioxide granules as an alternative to methyl bromide soil fumigation. Glob. J Agric Innov Res Dev. 2020 Nov;7:34–44. https://doi.org/10.15377/2409-9813.2020.07.5

Ristaino JB, Thomas W. Agriculture, methyl bromide, and the ozone hole: Can we fill the gaps? Plant Dis. 1997 Sep;81(9):964–977. https://doi.org/10.1094/PDIS.1997.81.9.964

Sánchez-Vallet A, Saleem-Batcha R, Kombrink A, Hansen G, Valkenburg DJ, Thomma BP, Mesters JR. Fungal effector Ecp6 outcompetes host immune receptor for chitin binding through intrachain LysM dimerization. Elife. 2013 Jul;2:e00790. https://doi.org/10.7554/eLife.00790

Song Y, Wilson AJ, Zhang XC, Thoms D, Sohrabi R, Song S, Geissmann Q, Liu Y, Walgren L, He SY, et al. FERONIA restricts *Pseudomonas* in the rhizosphere microbiome via regulation of reactive oxygen species. Nat Plants. 2021 May;7(5):644–654. https://doi.org/10.1038/s41477-021-00914-0

Staerck C, Gastebois A, Vandeputte P, Calenda A, Larcher G, Gillmann L, Papon N, Bouchara JP, Fleury MJJ. Microbial antioxidant defense enzymes. Microb Pathog. 2017 Sep;110:56–65. https://doi.org/10.1016/j.micpath.2017.06.015

Sun X, Zhou B, Luo Y, Ference C, Baldwin E, Harrison K, Bai J. Effect of controlled-release chlorine dioxide on the quality and safety of cherry/grape tomatoes. Food Control. 2017 Dec;82:26–30. https://doi.org/10.1016/j.foodcont.2017.06.021

R Core Team. A Language and environment for statistical computing. Vienna (Austria): R Foundation for Statistical Computing; 2013 [cited 2022 Oct 28]. Available from https://www.r-project.org

Trivedi P, Leach JE, Tringe SG, Sa T, Singh BK. Plant-microbiome interactions: from community assembly to plant health. Nat Rev Microbiol. 2020 Nov;18(11):607–621. https://doi.org/10.1038/s41579-020-0412-1

Vellend M. Conceptual synthesis in community ecology. Q Rev Biol. 2010 Jun;85(2):183–206. https://doi.org/10.1086/652373

Wahlberg I, Karlsson K, Austin DJ, Junker N, Roeraade J, Enzell CR, Johnson WH. Effects of flue-curing and ageing on the volatile, neutral and acidic constituents of Virginia tobacco. Phytochem. 1977;16(8):1217–1231. https://doi.org/10.1016/S0031-9422(00)94363-2

Wu T, Hu E, Xu S, Chen M, Guo P, Dai Z, Feng T, Zhou L, Tang W, Zhan L, et al. cluster Profiler 4.0: A universal enrichment tool for interpreting omics data. Innovation (Camb). 2021 Jul;2(3):100141. https://doi.org/10.1016/j.xinn.2021.100141

Yu G, Smith DK, Zhu H, Guan Y, Lam TTY. GGTREE: an R package for visualization and annotation of phylogenetic trees with their covariates and other associated data. Methods Ecol Evol. 2017 Jan; 8(1):28–36. https://doi.org/10.1111/2041-210X.12628

Zhang L, Wang X, Guo J, Xia Q, Zhao G, Zhou H, Xie F. Metabolic profiling of Chinese tobacco leaf of different geographical origins by GC-MS. J Agric Food Chem. 2013 Mar;61(11): 2597–2605. https://doi.org/10.1021/jf400428t

Zhong Y, Gan W, Du Y, Huang H, Wu Q, Xiang Y, Shang C, Yang X. Disinfection byproducts and their toxicity in wastewater effluents treated by the mixing oxidant of ClO_2/Cl_2. Water Res. 2019 Oct; 162: 471–481. https://doi.org/10.1016/j.watres.2019.07.012

Zimmer S, Messmer M, Haase T, Piepho HP, Mindermann A, Schulz H, Habekuß A, Ordon F, Wilbois KP, Heß J. Effects of soybean variety and *Bradyrhizobium* strains on yield, protein content and biological nitrogen fixation under cool growing conditions in Germany. Eur J Agron. 2016 Jan;72:38–46. https://doi.org/10.1016/j.eja.2015.09.008

Supplementary materials are available on the journal's website.